Nuclear Instruments and Methods in Physics Research A 797 (2015) 101–109

Contents lists available at ScienceDirect

Nuclear Instruments and Methods in Physics Research A

journal homepage: www.elsevier.com/locate/nima

Frequency pre-tuning of the niobium-sputtered quarter-wave resonator for HIE-ISOLDE project at CERN

P. Zhang [a,*], A. D'Elia [a,b,c,1], W. Venturini Delsolaro [a], K. Artoos [a]

[a] CERN, Geneva 23, Switzerland
[b] School of Physics and Astronomy, The University of Manchester, Oxford Road, Manchester M13 9PL, UK
[c] Cockcroft Institute of Science and Technology, Daresbury WA4 4AD, UK

ARTICLE INFO

Article history:
Received 18 May 2015
Received in revised form
23 June 2015
Accepted 24 June 2015
Available online 2 July 2015

Keywords:
Quarter-wave resonator
Frequency tuning
Niobium sputtering
HIE-ISOLDE

ABSTRACT

Superconducting quarter-wave resonators (QWRs) will be used in the superconducting linac upgrade in the frame of the HIE-ISOLDE project at CERN. The QWRs are made of bulk copper and have their inner surface covered with sputtered niobium. Their resonant frequency is 101.28 MHz at 4.5 K. Each cavity will be equipped with a tuning system to both minimize the forward power and compensate the frequency variations during production and beam operation. After a careful examination of all contributors to the frequency variation, we decomposed them into two components: frequency shift and its uncertainties. A pre-tuning step was subsequently added to the production sequence prior to niobium sputtering to accommodate the frequency shift mainly due to mechanical tolerances during substrate production, substrate surface treatment, niobium sputtering and cooldown process. To this end, the length of the QWR was chosen as a free parameter for the pre-tuning. Consequently the tuning system needs only to compensate the frequency uncertainties and Lorentz force detuning, thus its design has been largely simplified and its production cost was reduced by 80% comparing to its previous version. We have successfully applied this tuning scheme to five HIE-ISOLDE QWRs and the measured tuning error was 2.4 ± 1.9 kHz. This is well consistent with our calculations and well recoverable by the current simplified tuning system. It is worth noticing that the pre-tuning method only involves one-time measurement of the cavity's resonant frequency and its outer conductor length. This paper focuses on HIE-ISOLDE high-β QWR, but the method can be applied to HIE-ISOLDE low-β QWRs and other variants of QWR-like cavities.

1. Introduction

The High Intensity and Energy (HIE) ISOLDE project is a major upgrade of the existing post-accelerator facility at CERN [1]. The main focus is to boost the radioactive beam energy from 3 MeV/u to 10 MeV/u for a mass to charge ratio within $2.5 < A/q < 4.5$. This will be realized by replacing part of the existing normal conducting linac with superconducting quarter-wave resonators (QWRs) [2]. The QWRs will make use of the niobium (Nb) sputtered on copper (Cu) technology which was pioneered at CERN for LEP2 project [3] and subsequently developed at INFN-LNL to accommodate the complex QWR shape for the energy upgrade of ALPI project [4].

The HIE-ISOLDE QWR will be operated with a frequency of 101.28 MHz at 4.5 K. It will provide an accelerating gradient of 6 MV/m on beam axis with a maximum of 10 W power dissipation on the cavity inner surface. Two types of QWRs, low-β (6.3%) and high-β (10.3%), are planned to be installed in 3 phases to cover the entire energy range [5]. Since the linac upgrade started from the high energy section, all R&D efforts have been focussed on the high-β QWRs [6,7]. Its main parameters are listed in Table 1.

The production of a Nb-sputtered QWR requires several process steps [10] as shown in Fig. 1: Cu substrate production, substrate surface treatment, Nb sputtering and cavity cooldown to 4.5 K. The cavity resonant frequency evolves after each process and this needs to be characterized. We decomposed the frequency variation into two components: frequency shift and its uncertainties. The frequency shift is the frequency change from the copper QWR substrate to the Nb-coated cavity at operating frequency at 4.5 K, while the frequency uncertainties are the frequency fluctuations during each process. By analytical calculation, electromagnetic simulation and RF measurements, the frequency shift can be well determined, while the frequency uncertainties can be estimated.

Possessing a good knowledge of the frequency variation, a pre-tuning step was added to the overall tuning scheme. We used the cavity length as a free parameter to recover the frequency shift

* Corresponding author.
[1] Now at European Synchrotron Radiation Facility, Grenoble, France.

http://dx.doi.org/10.1016/j.nima.2015.06.039
0168-9002/

Table 1
The main parameters of the high-β QWR. The definitions are given in [8] and values are from [7,9].

Parameter	Value
f_0 at 4.5 K (MHz)	101.28
$\beta_{optimum}$ (%)	10.9
E_{peak}/E_{acc}	5.0
B_{peak}/E_{acc} (mT/(MV/m))	9.5
Geometry factor $G = R_s Q_0$ (Ω)	30.8
Nominal gradient E_{acc} (MV/m)	6
Nominal accelerating voltage V_{acc} (MV)	1.8
Power dissipation P_c at $E_{acc} = 6$ MV/m (W)	10
Q_0 at $E_{acc} = 6$ MV/m	4.7×10^8
Thickness of Nb layer (μm)	2–7
Thickness of Cu substrate (mm)	10

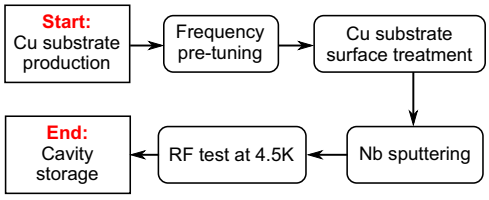

Fig. 1. A simplified QWR production workflow.

while using the tuning plate only to compensate the frequency uncertainties. As a consequence, the tuning system design has been largely simplified and the coarse tuning range is reduced from originally 220 kHz down to 42 kHz. This has been proved to be sufficient as long as the surface treatment scheme after substrate trimming is relatively stable. The most obvious benefit is the drastic fall of the tuning plate cost by 80% from its original version. The design and first test results of the simplified tuning system can be found in [7]. The measured frequency error of the pre-tuning for five QWRs is 2.4 ± 1.9 kHz. This can be well recovered by the tuning plate coarse range.

In this paper, all contributors to the frequency variations are carefully analyzed. Possessing a good knowledge of the frequency variation, a frequency tuning scheme is formulated with one pre-tuning step added. Finally the mechanism and the measured error of the frequency pre-tuning are described.

2. Variations of the cavity resonant frequency

The resonant frequency of a QWR can be varied by: manufacturing tolerances, surface treatment of the Cu substrate, Nb sputtering process, *RRR* of the sputtered Nb film, intrinsic quality factor of the cavity, cooldown process, presence of dielectrics in the cavity volume and eventually Lorentz force detuning. The impact of these contributors to the cavity frequency are described in detail along with measurement validations in this section. The parameters used for the following calculations are taken from Table 1.

2.1. Manufacturing tolerances

The geometry of a simplified QWR is shown in Fig. 2 together with geometry parameters relevant to the cavity frequency. The variation of these parameters alters the cavity resonant frequency. In order to evaluate the frequency sensitivity due to geometry changes, each cavity geometry parameter has been independently studied by ANSYS® HFSS simulations. The frequency convergence criterion is 400 Hz. The detailed explanation of this study can be found in [11]. The results are listed in Table 2. The most sensitive part is the length of the inner conductor (AntL). Unlike other

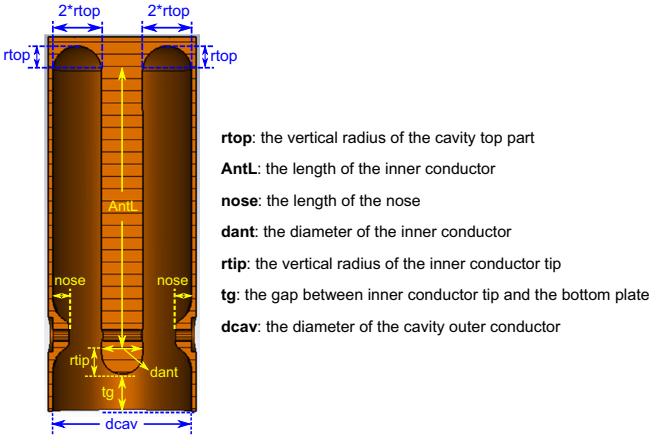

Fig. 2. The simplified model of a high-β QWR with main geometry parameter definitions.

Table 2
The frequency sensitivity to cavity geometry changes by +1 mm from the nominal value [11].

Geometry parameter	Δf (kHz/mm)
rtop	−105
AntL	−156
nose	−41
dant	−14
rtip	−107
tg	18
dcav	−24

parameters, a longer tip gap (tg) increases the cavity frequency. This is due to the decrease of the capacitance formed by the inner conductor tip and the bottom plate. The tip gap, in other words, the length of the cavity will be used as a free parameter to pre-tune the frequency. This will be explained in Section 4.

In the production of the Cu substrate, the manufacturing tolerance at the temperature of 20 °C and 50% relative humidity with normal pressure is required to be 0.1 mm for each geometry parameter. In the worst case where all errors add up, the frequency error due to manufacturing tolerances is calculated to be

$$\Delta F = \pm(105+156+41+14+107+18+24) \times 0.1 = \pm 46.5 \text{ kHz}. \quad (1)$$

This frequency error can be corrected by varying the tip gap by 2–3 mm by means of trimming the cavity outer conductor. The precision of trimming at CERN is 0.02 mm [12] which can be translated into approximately 400 Hz frequency uncertainty.

2.2. RRR of the sputtered Nb film

The quality of the sputtered Nb film varies from cavity to cavity. This will have an impact on the superconducting penetration depth and thus on the resonant frequency.

The penetration depth λ depends on temperature T and material properties and can be expressed as [13]

$$\lambda = \lambda_L \sqrt{1+\frac{\pi\xi_0}{2l}} \cdot \frac{1}{\sqrt{1-\left(\frac{T}{Tc}\right)^4}}, \quad (2)$$

$$\lambda_L = 32 \text{ nm}, \quad \xi_0 = 39 \text{ nm}, \quad (3)$$

where λ_L and ξ_0 are London penetration depth and BCS coherent length and their values are taken from the literature [14], the

electron mean free path l can be calculated from the residual resistance ratio RRR by [8]

$$l\,[\mathrm{nm}] = 2.7 \cdot RRR. \tag{4}$$

By using Eqs. (2) and (4), the variation of penetration depth due to dissimilar cavity RRR can be calculated. The change of penetration depth alters the cavity RF volume and consequently shifts the cavity resonant frequency. If we consider a perfect electric conducting (PEC) cavity with zero penetration depth at 4.5 K, the frequency variation Δf due to finite penetration depth can be calculated as [13]

$$\Delta f = f_{4.5\,\mathrm{K}} - f_{\lambda=0} = -\frac{\mu_0 \pi f_{4.5\,\mathrm{K}}^2}{G} \cdot (\lambda_{4.5\,\mathrm{K}} - 0). \tag{5}$$

The frequency variation from the PEC case as a function of the cavity RRR is shown in Fig. 3.

Small Cu and stainless-steel samples have been sputtered with Nb using the same sputtering parameters as for the cavities, and their RRR were measured. The values are ranging from 3 to 40 depending on sample locations on the cavity inner surface [9]. The overall RRR of the sputtered Nb film on the QWRs can vary from 5 to 60 [2], thus a frequency variation of 51 Hz can be expected as shown in Fig. 3.

2.3. Intrinsic quality factor of the cavity

The intrinsic quality factor, Q_0, of the Nb-sputtered QWR is specified to be 4.7×10^8 corresponding to a total power dissipation P_c of 10 W at nominal gradient 6 MV/m. However, the cavity will be operated with a bandwidth, Δf, of approximately 20 Hz to compensate the effect of microphonics. This corresponds to a loaded quality factor Q_L of

$$Q_L = \frac{f}{\Delta f} = \frac{101.28\ \mathrm{MHz}}{20\ \mathrm{Hz}} = 5.1 \times 10^6. \tag{6}$$

Therefore the external quality factor of the coupler, Q_{ext}, can be determined by

$$\frac{1}{Q_{ext}} = \frac{1}{Q_L} - \frac{1}{Q_0} = \frac{1}{5.12 \times 10^6}. \tag{7}$$

Since the pickup antenna used for the QWRs are highly undercoupled (Q_{ext} is beyond 10^{10}) and the insertion is fixed, we ignored the pickup contribution in the calculation.

The Q_0 of sputtered QWR varies from cavity to cavity [2]. In order to operate all cavities with a fixed bandwidth, the Q_{ext} of the coupler has to be changed to accommodate the dissimilar Q_0. This can be realized by changing the insertion of the input coupler. Fig. 4 shows the changes of coupler Q_{ext} due to cavity Q_0 variation for two different operation bandwidths. Within $\pm 50\%$ of P_c changes asked by Q_0 changes, the Q_{ext} variations are small for both bandwidths.

The insertion of the coupler changes the coupler Q_{ext} and the cavity resonant frequency as shown in Fig. 5. For an operating bandwidth of 20 Hz, the desired Q_{ext} requires a coupler insertion of approximately 8.6 mm, which corresponds to a frequency perturbation of -1.2 kHz as seen in Fig. 6. The Q_0-induced ($\pm 50\%$ of nominal P_c) Q_{ext} variations shown in Fig. 4(b) will require small changes of the coupler insertion, thus alter the frequency perturbation by ± 20 Hz.

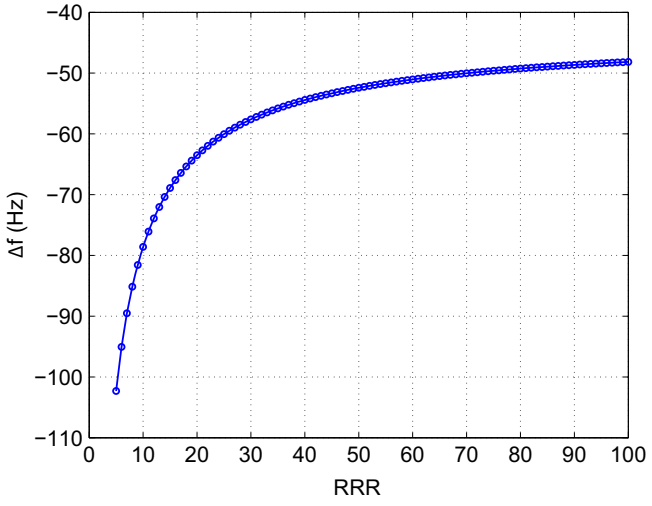

Fig. 3. The frequency deviation from a perfect conducting cavity case (zero penetration depth) as a function of RRR.

2.4. Cooldown process

The cool down of the QWR from room temperature to 4.5 K in vacuum will alter the resonant frequency due to the thermal contraction of the cavity geometry. The ambient environment changes from normal air (293 K, 50% relative humidity with normal pressure) to vacuum, and the surface impedance changes from normal conducting Cu to superconducting Nb also modify the resonant frequency. The substrate was made of Cu-OFE UNS C10100 with a minimum RRR of 100. The inner conductor and the outer conductor were machined separately from 3D-forged half-hard Cu billets, then assembled by shrink fit, and finally electron beam welded from the RF side. The details on Cu substrate production can be found in [15].

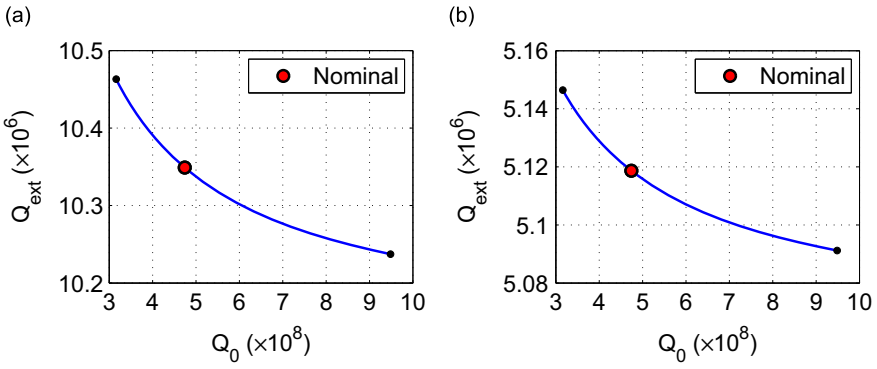

Fig. 4. Q_{ext} of the coupler as a function of cavity Q_0 for two different operation bandwidths: (a) 10 Hz and (b) 20 Hz.

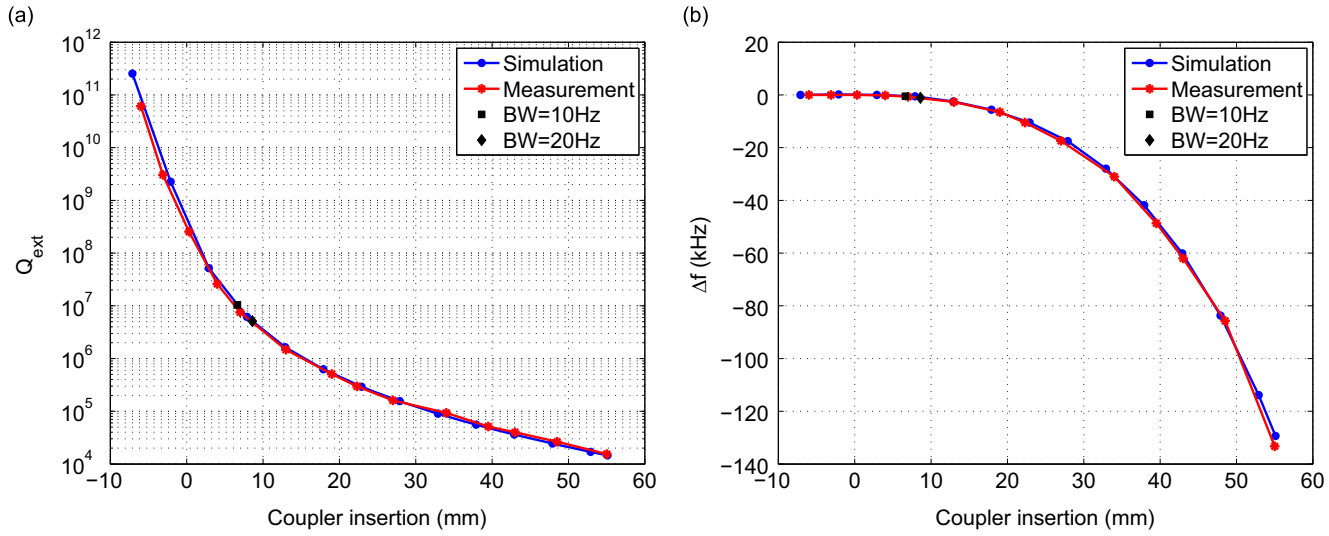

Fig. 5. (a) Q_{ext} of the coupler as a function of its insertion. (b) The perturbation to the cavity resonant frequency as a function of coupler insertion.

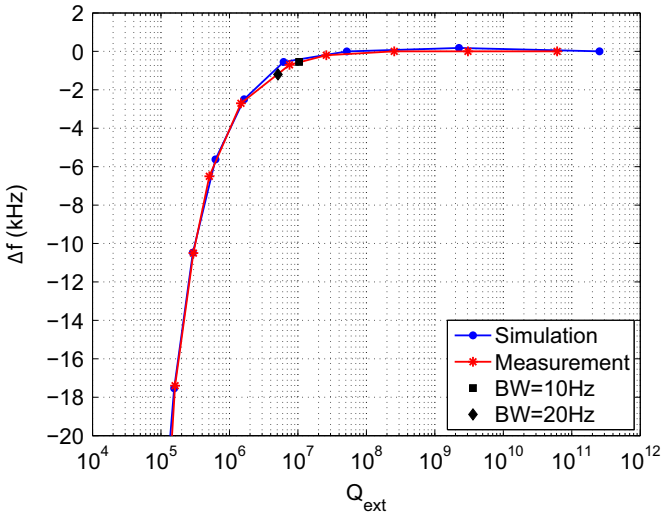

Fig. 6. The frequency perturbation as a function of the coupler Q_{ext} due to coupler insertion changes.

2.4.1. Thermal contraction

The cavity resonant frequency f changes with thermal expansion of the cavity, and is inversely proportional to the linear dimension L of the cavity,

$$f = C \cdot \frac{1}{L}, \tag{8}$$

where C is a constant. The frequency shift Δf due to thermal expansion can thus be obtained by using Eq. (8),

$$\frac{\Delta f}{f} = -\frac{\Delta L}{L}. \tag{9}$$

We used the data from [16] to determine the integrated dimension variation of Cu as

$$\frac{\Delta L}{L} = \int_{4.5\ \mathrm{K}}^{293\ \mathrm{K}} \alpha(t)\, dt = 0.3247\%. \tag{10}$$

Therefore the frequency shift from 4.5 K to 293 K due to thermal expansion is

$$\Delta f_{\mathrm{thermal}} = -0.3247\% \times 101.28\ \mathrm{MHz} = -328.9\ \mathrm{kHz}. \tag{11}$$

This is the dominate term of the total frequency shift.

2.4.2. Ambient environment

The change of ambient environment from normal air to vacuum at 4.5 K alters the relative electric permittivity ϵ_r. Knowing the cavity frequency in vacuum, the frequency in air can then be calculated as

$$f_{\mathrm{air}} = \frac{1}{\sqrt{\epsilon_0 \epsilon_r \mu_0}\lambda_{vac}} = \frac{f_{\mathrm{vac}}}{\sqrt{\epsilon_r}}, \tag{12}$$

where λ_{vac} is the wavelength in vacuum and ϵ_r of air is given by [17]

$$(\epsilon_r - 1)\cdot 10^6 = 210\frac{P_a}{T} + 180\left(1 + \frac{5580}{T}\right)\frac{P_w}{T}, \tag{13}$$

where T is the absolute temperature in K, P_a and P_w are vapor pressures of air and water in mm Hg and can be expressed as [18],

$$P_w = h \times 10^{(8.07131 - (1730.63/(233.426+T))}, \tag{14}$$

$$P_a = 760 - P_w, \tag{15}$$

where h is the relative humidity of the air. In our case, the ϵ_r for air at 20 °C and 50% relative humidity with normal pressure is calculated to be 1.000647. Therefore the frequency shift from vacuum to air is

$$f_{\mathrm{air}} - f_{\mathrm{vac}} = 101.28\ \mathrm{MHz} \times \left(\frac{1}{\sqrt{\epsilon_r}} - 1\right) = -32.7\ \mathrm{kHz}. \tag{16}$$

2.4.3. Surface impedance

The surface impedance of Cu at room temperature and Nb at 4.5 K is different and this can cause a frequency variation between warm and cold measurement.

The surface impedance and the cavity resonant frequency can be related as [19,20],

$$\frac{1}{Q_0} - 2j\frac{\Delta\omega}{\omega_0} = \frac{R_s + jX_s}{G}, \tag{17}$$

where R_s and X_s are surface resistance and surface reactance, ω_0 is the unperturbed frequency considering zero penetration depth hence zero surface impedance, $\Delta\omega$ is the frequency shift due to finite surface reactance, G is the cavity geometry factor. Thus we can obtain the following equation relating surface reactance and frequency shift as

$$X_s = -2G\frac{\Delta\omega}{\omega_0}. \tag{18}$$

The surface reactance for superconductors [8] and normal conductors [21] are

$$X_s^{SC} = -2G\frac{\omega_{sc}-\omega_0}{\omega_0} = \omega_{sc}\mu_0\lambda, \tag{19}$$

$$X_s^{NC} = -2G\frac{\omega_{nc}-\omega_0}{\omega_0} = \omega_{nc}\mu_0\frac{\delta}{2}, \tag{20}$$

where λ is the penetration depth defined in Eq. (2), δ is the skin depth [21]. Therefore the frequency shift can be obtained from Eqs. (19) and (20) as

$$\Delta\omega = \omega_{nc}-\omega_{sc} = \frac{\mu_0\omega_{sc}^2\left(\lambda-\frac{\delta}{2}\right)}{2G-\mu_0\omega_{sc}\left(\lambda-\frac{\delta}{2}\right)}. \tag{21}$$

We use the parameter values in Table 1, $RRR = 15$ [2] and $\delta = 6.6\,\mu$m for Cu at 293 K, the frequency shift from Nb-sputtered superconducting cavity to normal conducting Cu substrate due to surface reactance variations is -4.3 kHz.

The total frequency shift during the cooldown process from 293 K and 50% relative humidity with normal pressure in air to 4.5 K in vacuum is

$$\Delta f_{\text{cooldown}} = 328.9+32.7+4.3 = 365.9\ \text{kHz}. \tag{22}$$

The measured frequency shift during the cooldown process is shown in Fig. 7. The average frequency shift is measured to be 370.5 kHz with a peak-to-peak uncertainty of 6 kHz. This is consistent with the calculated value in Eq. (22).

2.5. Substrate surface treatment and Nb sputtering process

The Cu substrate was degreased and chemically etched in order to prepare the Cu surface before Nb sputtering. The chemical etching agent (SUBU) is a mixture of sulfamic acid, hydrogen peroxide, *n*-butanol and ammonium citrate at a temperature of 72 °C. The effectiveness of SUBU was previously studied at CERN. The average roughness R_a reached 0.8 μm after 20 μm removal on the surface. This accounts for a SUBU duration of approximately 30 min. The details of SUBU and the production process for HIE-ISOLDE QWRs can be found in [10,22]. The QWR was subsequently sputtered with Nb at high temperature: 315–625 °C for the inner conductor corresponding to 300–435 °C for the outer conductor [23].

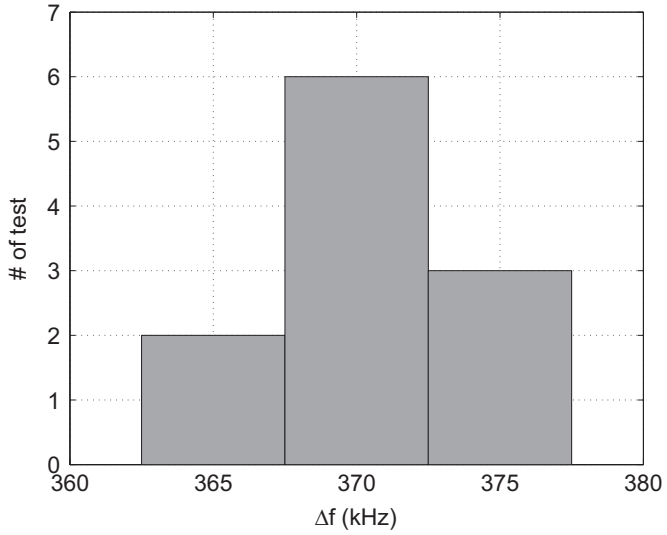

Fig. 7. The measured frequency shift from 293 K and 50% relative humidity air with normal pressure to 4.5 K in vacuum.

The cavity frequency was carefully monitored between each surface treatment step and finally after the Nb sputtering. As shown in Fig. 8, the frequency variation has a linear-like dependence on the SUBU duration. The cavity will lose 26.5 kHz after 40-min SUBU etching while the Nb sputtering process brings its frequency further down by 6.8 kHz. The corresponding frequency shift and its uncertainty are listed in Table 3.

2.6. Lorentz force detuning

The Lorentz force detuning [24] of the Nb-sputtered-on-Cu QWR is very small because of the considerably thicker wall of the Cu substrate ($\sim$10 mm). The dominant contribution is from the tuning plate which is normally much thinner than 10 mm. As will be described in Section 3, the new simplified tuning plate has a deformable part of only 0.3 mm thick. Fig. 9 shows the electric and magnetic field distributions of the QWR at its lower part. The Lorentz force pulls the tuning plate towards the inner conductor tip and thus lower the cavity resonant frequency. Fig. 10 shows the frequency detuning by Lorentz force measured at various cavity gradient at 4.5 K. At nominal gradient ($E_{acc} = 6$ MV/m), the cavity resonant frequency is detuned by -350 Hz when the tuning plate was disconnected from the lever system [7] therefore being left free. This corresponds to a detuning coefficient of $\kappa = -9.1$ Hz/(MV/m)^2, which is very comparable to the previous measurements using the original tuning plate [25]. Once the lever system is connected to the plate, the frequency detuning is largely reduced to -110 Hz ($\kappa = -3.0$ Hz/(MV/m)^2) when the tuning plate is at flat position and even down to -50 Hz ($\kappa = -1.3$ Hz/(MV/m)^2 when the plate is pulled to the mid-range position ($\sim$2.5 mm deformation from the flat position). This is because that all QWRs need to be tuned to 101.28 MHz at cold by pulling the plate away from the inner conductor tip. This mitigates the Lorentz force on the plate resulting in less frequency detuning.

The frequency detuning will vary slightly from cavity to cavity due to different tip gap value determined in the pre-tuning step (see Section 4). In addition, the position where the tuning plate is

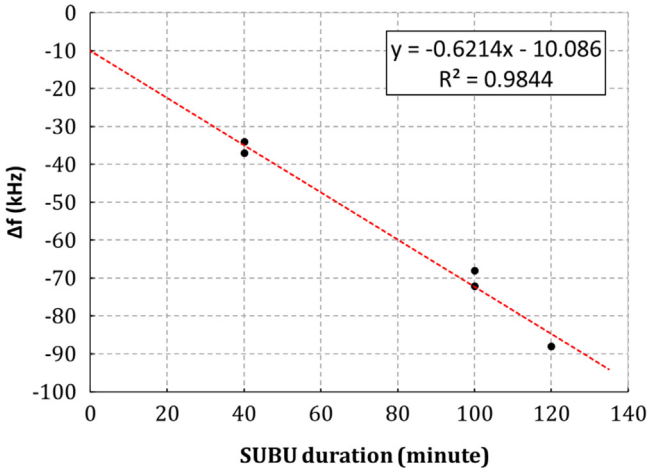

Fig. 8. The measured frequency shift as a function of SUBU duration.

Table 3
The measured frequency variation due to SUBU and Nb sputtering.

Process name	**Frequency shift (kHz)**
40-min SUBU	26.5 ∓ 3.0
Nb sputtering	6.8 ∓ 3.3

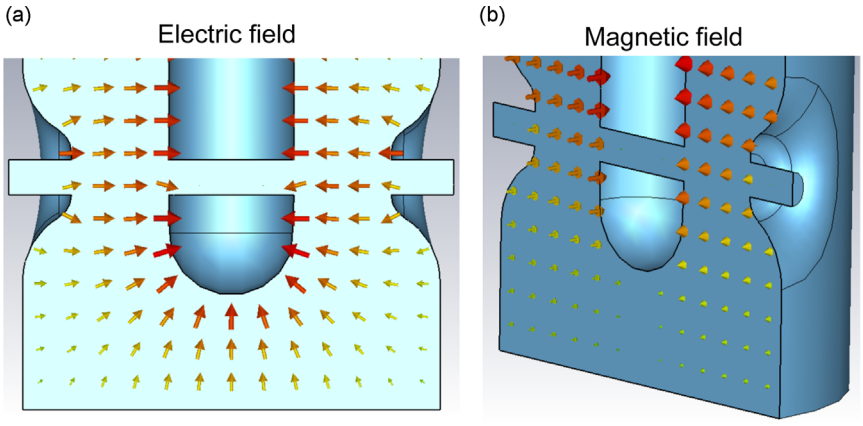

Fig. 9. The electric and magnetic field distribution of the QWR simulated using CST Microwave Studio®.

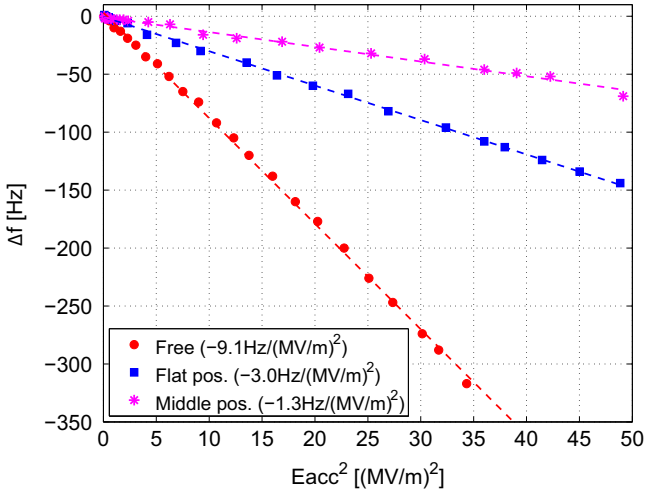

Fig. 10. The Lorentz force detuning of QWR measured at cold with the tuning plate at different conditions. The dashed curves are fitted linearly with respect to the E_{acc}.

deformed to in order to reach 101.28 MHz at cold will not be the same for all cavities, therefore exerts dissimilar mitigation force on the plate. This will also lead to slightly different frequency detuning. The frequency detuning due to Lorentz force is approximately −100 Hz and can be well compensated by the tuning range at cold. The hysteresis and tuning resolution have been measured at cold and reported in [7].

At this stage, all contributors to the frequency variations of the QWR have been described and their impact on the cavity frequency have been characterized and summarized in Table 4. Once the cavity has been pre-tuned by trimming the outer conductor, all subsequent processes will reduce the cavity frequency. Thus a suitable frequency margin has to be reserved in the pre-tuning step. In this case, the tuning system will only need to compensate the "f_0 error"s as shown in Table 4. These errors are estimated to be less than 10 kHz in total.

3. The tuning system

The original tuning system is conceptually similar to TRIUMF's and was described in [6]. An oilcan shaped diaphragm of copper–beryllium (CuBe) was hydroformed and then sputtered with Nb as shown in Fig. 11(a). The tuning coarse range is 220 kHz, which is more than 20 times of the expected frequency error. This is highly costly and not necessary. Therefore a simplified tuning plate has been designed in year 2013 as shown in Fig. 11(b). The plate is

Table 4
The frequency shift and uncertainties of the QWR.

Contributors	**Value (kHz)**	**Type**
Manufacturing error (max)	±46.5	f_0 shift
Surface treatment (40' SUBU)	−26.5	f_0 shift
Nb sputtering process	−6.8	f_0 shift
Cooldown process	−370.5	f_0 shift
Q_0 of the Nb-sputtered QWR	−1.2	f_0 shift
Trimming at CERN	0.4	f_0 error
RRR of the Nb film	0.05	f_0 error
Q_0 of the Nb-sputtered QWR	0.02	f_0 error
Cooldown process	6	f_0 error
Surface treatment (40' SUBU)	3.0	f_0 error
Nb sputtering process	3.3	f_0 error
Lorentz force detuning	−0.1	f_0 error

machined from a flat Cu OFE plate and sputtered with Nb. The tuning is realized by deforming the plate from the center, where the deformable part is 0.3 mm thick. The plate can be deformed up to 5 mm from the flat position and can still maintain its elasticity. The coarse tuning range can reach 42 kHz, well enough to cover the expected ~10 kHz frequency error. The detailed explanation of the current tuning system can be found in [7].

4. Cavity frequency pre-tuning

All QWRs are initially produced with a fixed and longer-than-needed tip gap. The aim of the pre-tuning is to tune the cavity frequency to a previously determined target frequency by trimming the cavity outer conductor. In this section we will describe how to determine the tuning target frequency and details the tuning mechanism. Finally the frequency errors for all five pre-tuned QWRs are given.

4.1. The target frequency at room temperature

The working frequency of the QWR is 101.28 MHz at 4.5 K under vacuum with the tuning plate preferably pulled to its mid-range position. However, the tuning measurement is conducted with a flat plate in the metrology lab where temperature and humidity are regulated. Therefore the target frequency for tuning has to be scaled. Fig. 12 shows the step-by-step scaling of the cavity frequency. Considering a 40 kHz coarse range, this will bring down the frequency by 20 kHz by releasing the tuning plate from its previously pulled mid-range position to a flat position. Since the frequency was measured at room temperature during the pre-tuning step, the frequency needs to be scaled by −370 kHz to

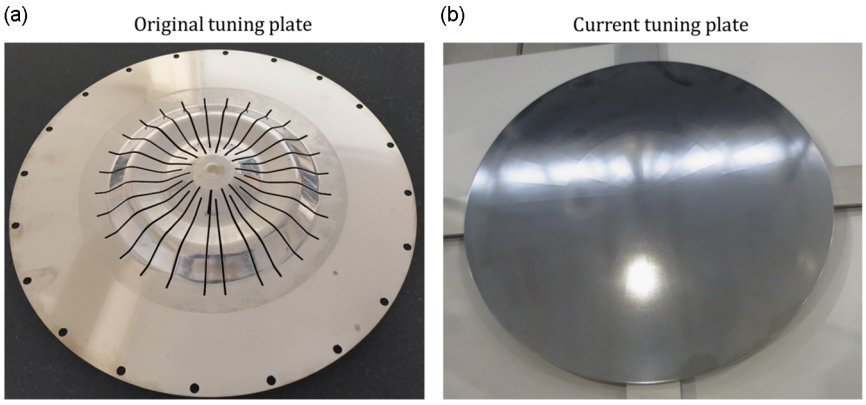

Fig. 11. The original and the current tuning plate for high-β QWRs.

f_0(MHz)	Δf	Ambient environment	Tuning plate position	Pickup installed?
101.280		Vacuum at 4.5K	Middle	No
	-20 kHz	Middle position → flat position		
101.260		Vacuum at 4.5K	Flat	No
	-370 kHz	Vacuum at 4.5K → Air at 293K, 50% humidity		
100.890		Air at 293K, 50% humidity	Flat	No
	-27 kHz	Pickup perturbation		
100.863		Target frequency at room temperature	Flat	Yes

Fig. 12. The target frequency at room temperature.

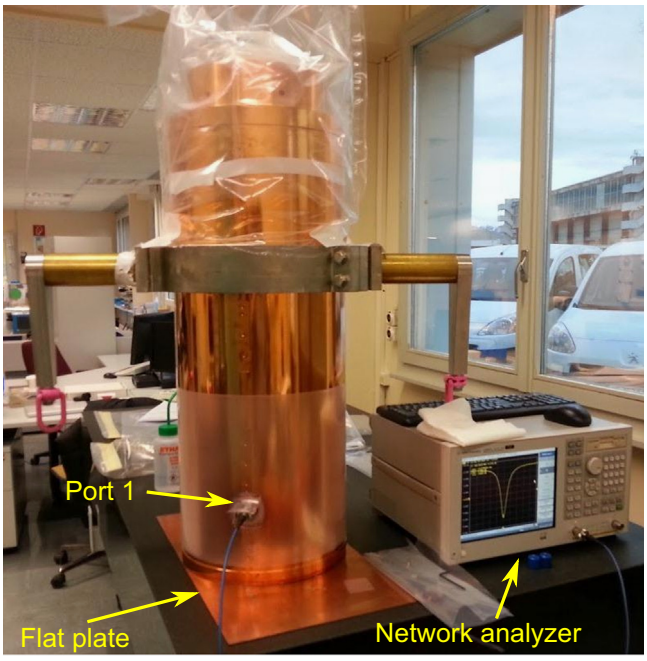

Fig. 13. The setup for the frequency measurement.

accommodate the changes due to warm-up process as described in Section 2.4.

The measurement of the cavity resonant frequency at warm is conducted by measuring the scattering parameter S_{11} in the metrology lab at CERN where the ambient temperature and humidity are regulated. A typical measurement setup is shown in Fig. 13. The cavity is closed by a flat Cu plate at the bottom. The weight of the cavity itself (larger than 100 kg) ensures a good RF contact. The frequency is measured by using a simple stainless

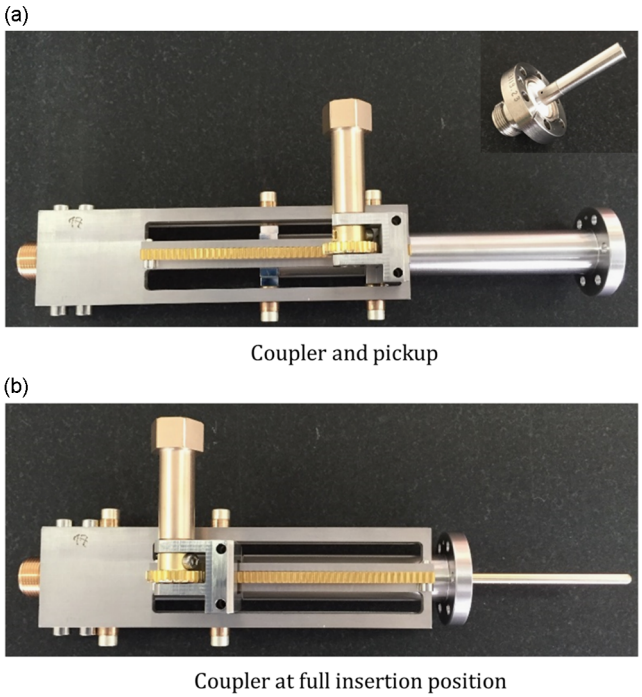

Fig. 14. The mobile coupler and pickup. (a) Coupler and pickup. (b) Coupler at full insertion position.

steel pickup antenna as shown in Fig. 14(a). Before performing the frequency measurement it is important to assure that the cavity is and remains in thermal equilibrium with the environment. This is essential to avoid frequency measurement errors.

The insertion of the pickup antenna changes the capacitance from the cavity inner conductor to the pickup end, therefore alters the cavity resonant frequency. This pickup-induced frequency perturbation has to be characterized. This was done, in absence of pickup antenna, by using a mobile coupler where the insertion of the coupler inner conductor can be changed as shown in Fig. 14. By reducing the insertion, the coupler perturbation decreases, hence the cavity frequency increases as shown in Fig. 15. After pulling out the coupler inner pin by 28 gear turns, the frequency stops increasing, and this is the unperturbed cavity frequency. Comparing it to the frequency measured by using the pickup antenna, the frequency perturbation of the pickup antenna is determined to be −27 kHz. This is used in the frequency scaling in Fig. 12.

Finally the target frequency for tuning at warm is determined to be 100.863 MHz. Since the frequency varies both with temperature and humidity changes of the ambient environment, these

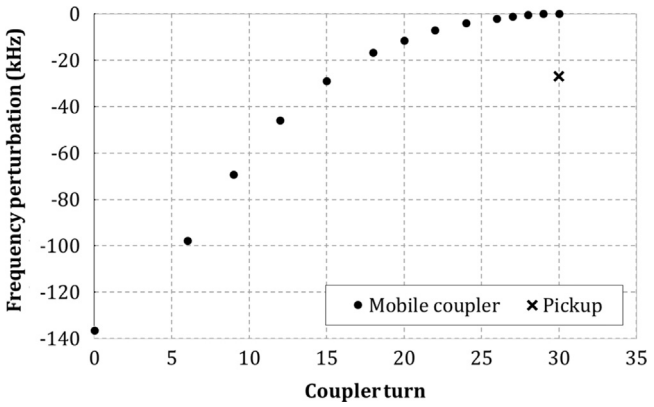

Fig. 15. The frequency perturbation of the pickup and mobile coupler.

effects have also been calculated by using equations listed in Section 2.4.2 and are shown in Table 5. The cavity will lose 1.7 kHz by increasing the ambient temperature by 1 °C, and approximately 1 kHz by increasing the relative humidity by 10%.

4.2. The tuning mechanism

As described in previous sections,"tip gap" is the free parameter for pre-tuning. Given a target frequency, the desired tip gap will be different from cavity to cavity due to mechanical tolerance and SUBU duration to be conducted after substrate trimming (see Fig. 1). For a newly produced cavity, the desired tip gap can be determined by a one-time measurement of initial cavity frequency and initial tip gap value along with the previously determined reference curve and target frequency at warm.

Taking the cavity QS2.1[2] as an example, the reference curve is the cavity frequency response to tip gap variations and has been previously determined by electromagnetic simulations. This is the black dot curve in Fig. 16. The initial tip gap of QS2.1 was measured to be 107.7 mm and the measured frequency was 101.206 MHz after 24 h of thermalization in metrology lab and normalized to 20 °C and 50% relative humidity using Table 5. This is shown in Fig. 16 as the red solid dot. Moving down the calibration curve until it intersects the initial measured point, the blue solid curve is the working curve for QS2.1. This curve describes the cavity frequency response to different tip gap values for QS2.1. The ideal target frequency has been previously determined to be 100.863 MHz considering no further frequency shift by surface treatment and sputtering process. This is denoted as the black dashed line. The intersection of the working curve and the ideal target frequency line is the suggested ideal point and is denoted by the solid green square.

Based on the optical inspection of the cavity inner surface, we decided to undertake 100-min SUBU after trimming followed by the Nb sputtering. According to Fig. 8, these steps will shift the frequency down by 72 kHz. This has to be reserved during the pre-tuning thus making the final tuning target to be 100.936 MHz. This is shown in Fig. 16 by the magenta dash-dot line. Therefore the final suggested tuning point is denoted as the solid magenta hexagram. The suggested tip gap is 82.0 mm, thus needs a trimming of 25.7 mm from the initial tip gap value of 107.7 mm.

After trimming, surface treatment and Nb sputtering, the cavity frequency was measured again at room temperature. The total frequency drop is measured to be 68 kHz. Thus the tuning error for QS2.1 is 4 kHz. According to Table 4, the tuning error is originated from trimming error, RRR of the Nb film, surface treatment and Nb sputtering process. This can be calculated as [26]

$$\sqrt{0.4^2+0.051^2+\left(3.0\cdot\frac{100\ \text{min}}{40\ \text{min}}\right)^2+3.3^2}=8.2\ \text{kHz}. \quad (23)$$

The measured tuning error is consistent with the calculated value. At this stage, we conclude that the pre-tuning of QS2.1 is complete.

By using this pre-tuning method, we have successfully tuned five QWRs and the average tuning error is 2.4 ± 1.9 kHz. Together with a maximum measured cooldown process error of 3.5 kHz, the total frequency error can be well recovered by the tuning plate coarse range.

[2] The naming conventions for HIE-ISOLDE QWRs can be found in [2].

Table 5
The impact of temperature and humidity variations on cavity frequency.

Item name	Δf (kHz)
Temperature ±1 K from 293 K	±1.7
Humidity $\pm10\%$ from 50%	±1

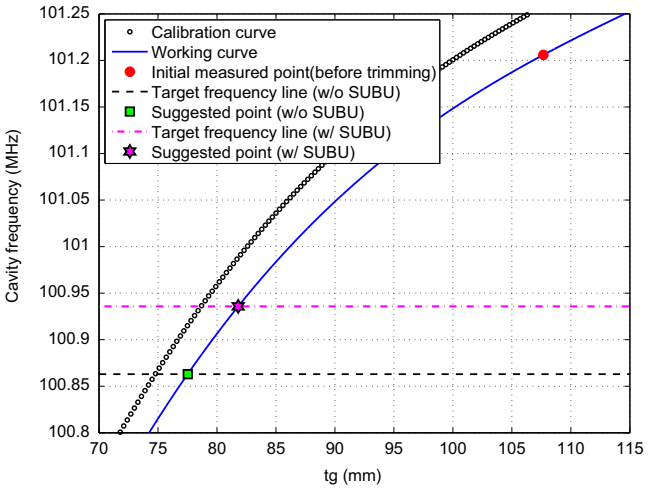

Fig. 16. The tuning mechanism. (For interpretation of the references to color in this figure caption, the reader is referred to the web version of this paper.)

5. Final remarks

The causes of the frequency variation for HIE-ISOLDE high-β QWRs have been fully analyzed and decomposed into well-determined frequency shift and carefully estimated frequency uncertainties. Based on this information, a new tuning scheme has been made. A pre-tuning step has been added prior to Nb sputtering in order to accommodate the already-determined frequency shift by using the cavity length as a free parameter. On the other hand, the tuning system only needs to compensate the frequency uncertainties which has been estimated to be rather small (less than 10 kHz). This has led to a large simplification of the tuning system design and consequently reduced the production cost of the tuning plate by 80% from its original version.

A total of five HIE-ISOLDE high-β QWRs have been tuned by this tuning scheme and the tuning error for all five cavities was measured to be less than 5 kHz. This is in accordance with the calculations and can be well recovered by the 42 kHz coarse range of the current tuning system.

One needs to notice that the pre-tuning method only requires one-time measurement of the cavity frequency and the cavity length. Moreover the method can be easily applied on HIE-ISOLDE low-β QWRs and other QWR-like cavities.

Acknowledgments

We thank M. Therasse, G. Pechaud and M. Gourragne for their help in preparing the measurements. Thanks to S. Aull, R. Torres-Sanchez and A. Sublet for very useful discussions. This work has been supported partly by a Marie Curie Early Initial Training Network Fellowship of the European Community's 7th Programme under contract number PITN-GA-2010-264330-CATHI.

References

[1] W. Venturini, et al., in: Proceedings of LINAC2014, Geneva, Switzerland, pp. 795–800.
[2] W. Venturini Delsolaro, et al., in: Proceedings of SRF2013, Paris, France, pp. 767–772.
[3] S. Calatroni, J. Phys. Conf. Ser. 114 (2008) 12006.
[4] A.M. Porcellato, et al., Pramana J. Phys. 59 (2002) 871.
[5] M. Pasini, et al., in: Proceedings of SRF2009, Berlin, Germany, pp. 924–929.
[6] A. D'Elia, et al., in: Proceedings of SRF2009, Berlin, Germany, pp. 609–613.
[7] P. Zhang, et al., in: Proceedings of SRF2013, Paris, France, pp. 1121–1125.
[8] H. Padamsee, J. Knobloch, T. Hays, RF Superconductivity for Accelerators, second edition, Wiley-VCH, ⟨http://eu.wiley.com/WileyCDA/WileyTitle/productCd-3527408428.html#⟩.
[9] A. Sublet, et al., in: Proceedings of SRF2013, Paris, France, pp. 620–622, ⟨http://store.elsevier.com/product.jsp?isbn=9780750672917&pagename=search⟩.
[10] M. Therasse, et al., in: Proceedings of LINAC2014, Geneva, Switzerland, pp. 1165–1167.
[11] P. Zhang, et al., Frequency Sensitivity to Cavity Geometry Errors of HIE-ISOLDE High-Beta Quarter-Wave Resonator, CERN Note: CERN-ACC-NOTE-2014-0022, 2014.
[12] K. Artoos, private communication, 2015.
[13] T. Junginger, Investigation of the surface resistance of superconducting materials (Ph.D. thesis).
[14] E. Maxwell, P.M. Marcus, J.C. Slater, J. Supercond. 4 (1991) 341.
[15] L. Alberty, et al., in: Proceedings of SRF2013, Paris, France, pp. 596–598.
[16] N.J. Simon, E.S. Drexler, R.P. Reed, Properties of Copper and Copper Alloys at Cryogenic Temperature, NIST Monograph.
[17] M.E. Van Valkenburg, W.M. Middleton, Reference Data for Engineers: Radio Electronics, Computer, and Communications, ninth edition, Newnes.
[18] B.E. Poling, J.M. Prausnitz, J.P. O'Connell, The Properties of Gases and Liquids, fifth edition, McGraw-Hill Professional, ⟨http://www.amazon.com/Properties-Gases-Liquids-Bruce-Poling/dp/0070116822⟩.
[19] E. Maxwell, P.M. Marcus, J.C. Slater, Phys. Rev. 76 (1949) 1332.
[20] A. D'Elia, Frequency Scaling from Copper to SC Niobium, HIE-ISOLDE Note: HIE-ISOLDE-PROJECT-Note-0007, 2010.
[21] D.M. Pozar, Microwave Engineering, fourth edition, Wiley, ⟨http://eu.wiley.com/WileyCDA/WileyTitle/productCd-EHEP002016.html⟩.
[22] G. Lanza, et al., in: Proceedings of SRF2009, Berlin, Germany, pp. 801–805.
[23] N. Jecklin, et al., in: Proceedings of SRF2013, Paris, France, pp. 611–613.
[24] E. Häbel, J. Tückmantel, Electromagnetic surface forces in RF cavities, CERN Note: CERN-AT-RF-INT-91-99, 1991.
[25] S. Calatroni, et al., in: Proceedings of LINAC2010, Tsukuba, Japan, pp. 827–829.
[26] H. Ku, J. Res. Nat. Bur. Stand. Sec. C: Eng. Inst. 70C (1966) 263.